Article

Current Biology

Convergence of vestibular and proprioceptive signals in the cerebellar nodulus/uvula enhances the encoding of self-motion in primates

Highlights

- Vestibular-sensitive Purkinje cells also robustly encode proprioceptive input
- Vestibular and proprioceptive tuning of Purkinje cells is aligned to enhance coding
- Proprioceptive cues of head position shape Purkinje cell vestibular responses
- Populations of Purkinje cells compute head and body motion in space

Authors

Robyn L. Mildren, Lex J. Gómez, Kathleen E. Cullen

Correspondence

kathleen.cullen@jhu.edu

In brief

The cerebellar nodulus/uvula (NU) is known to be a critical hub for integrating vestibular signals from the canals and otoliths to stabilize gaze and maintain spatial orientation relative to gravity. Mildren et al. reveal that NU Purkinje cells also dynamically integrate proprioceptive with vestibular input to stabilize posture relative to space.

Mildren et al., 2025, Current Biology *35*, 1–15
February 3, 2025
https://doi.org/10.1016/j.cub.2024.11.063

CellPress

Please cite this article in press as: Mildren et al., Convergence of vestibular and proprioceptive signals in the cerebellar nodulus/uvula enhances the encoding of self-motion in primates, Current Biology (2024), https://doi.org/10.1016/j.cub.2024.11.063

Current Biology

CellPress

Article

Convergence of vestibular and proprioceptive signals in the cerebellar nodulus/uvula enhances the encoding of self-motion in primates

Robyn L. Mildren,[1] Lex J. Gómez,[1] and Kathleen E. Cullen[1,2,3,*]
[1]Johns Hopkins University, Department of Biomedical Engineering, 720 Rutland Avenue, Baltimore 21205, USA
[2]X (formerly Twitter): @TheCullenLab
[3]Lead contact
*Correspondence: kathleen.cullen@jhu.edu
https://doi.org/10.1016/j.cub.2024.11.063

SUMMARY

The integration of different sensory streams is required to dynamically estimate how our head and body are oriented and moving relative to gravity. This process is essential to continuously maintain stable postural control, autonomic regulation, and self-motion perception. The nodulus/uvula (NU) in the posterior cerebellar vermis is known to integrate canal and otolith vestibular input to signal angular and linear head motion in relation to gravity. However, estimating body orientation and motion requires integrating proprioceptive cues with vestibular signals. Lesion studies demonstrate that the NU is crucial for maintaining postural control, suggesting it could play an important role in combining multimodal sensory input. Using high-density extracellular recordings in rhesus monkeys, we found that the majority of vestibular-sensitive Purkinje cells also encoded dynamic neck proprioceptive input. Furthermore, Purkinje cells generally aligned their directional tuning to vestibular and proprioceptive stimulation such that self-motion encoding was enhanced. The heterogeneous response dynamics among Purkinje cells enabled their population activity to generate head or body motion encoding in the downstream nuclei neurons on which they converge. Strikingly, when we then experimentally altered the orientation of the head relative to the body, Purkinje cells modulated their responses to vestibular stimulation to account for the change in body motion in space. These findings reveal that the NU integrates proprioceptive and vestibular input synergistically to maintain robust postural control.

INTRODUCTION

The brain continuously integrates different streams of sensory information to dynamically estimate the orientation and motion of our head and body relative to gravity. This computation is essential to maintain stable postural control, autonomic regulation, and self-motion perception. Importantly, the vestibular system senses gravity and motion of the head in space, which is used by the brain to stabilize gaze and maintain head and body posture across vertebrates.[1–3] One major hub of vestibular processing is the nodulus/uvula (NU) in the cerebellar vermis (lobules X and IX). The NU is not only heavily interconnected with neurons in the brainstem vestibular nuclei, which comprise the first central stage of vestibular processing,[4–11] but it is also the only region of the cerebellum that receives direct input from primary vestibular canal and otolith afferents (monkey[12] and mouse[13]). The classic view is that the function of the NU is to integrate angular and linear motion signals from the semicircular canals and otoliths to represent the orientation and motion of the head relative to gravity.[14,15] This view is supported by studies on gaze stabilization following NU lesions[16,17] as well as single-unit recordings of NU Purkinje cells during vestibular stimulation induced by passive whole-body motion.[18–20]

However, in addition to its role in gaze stabilization via the vestibuloocular reflex (VOR),[16,17] studies in human patients indicate that the NU also plays an essential role in stabilizing posture. Specifically, selective damage to the NU results in severe impairments in head and body postural control, which are more pronounced than those observed for the VOR (humans[21–24]; monkeys[25]). Importantly, generating appropriate vestibular postural responses requires the brain to rapidly integrate multiple streams of sensory feedback to account for the position and movement of the body relative to the head—the native reference frame of the vestibular organs. The outcome of this sensory integration is demonstrated by studies showing that human postural reflexes evoked by galvanic vestibular stimulation are modulated by sensory feedback about head-on-body position.[26–28] This transformation of vestibular postural responses critically relies upon neck proprioceptive cues.[29] Consequently, a fundamental question arises: does the NU integrate multiple sensory modalities, proprioceptive and vestibular, to compute an estimate of body motion relative to gravity?

Accordingly, here we directly tested the hypothesis that the NU of the cerebellum integrates neck proprioceptive cues with vestibular input by conducting high-density extracellular recordings from individual NU Purkinje cells, the output neurons of the

Please cite this article in press as: Mildren et al., Convergence of vestibular and proprioceptive signals in the cerebellar nodulus/uvula enhances the encoding of self-motion in primates, Current Biology (2024), https://doi.org/10.1016/j.cub.2024.11.063

cerebellar cortex, in rhesus monkeys. Our analysis of simple spike activity revealed that the vast majority of vestibular-sensitive Purkinje cells also robustly encoded dynamic neck proprioceptive input. Purkinje cells aligned the directional tuning of their vestibular and proprioceptive responses to generate an overall enhanced encoding of self-motion. Furthermore, their heterogeneous response dynamics enabled the combined activity of a Purkinje cell population to signal either pure head or body motion to the output nuclei of the cerebellum. Importantly, when we then altered the orientation of the head relative to the body, Purkinje cells modulated their response to the same otolith stimulation in order to account for the change in body motion in space. Our findings reveal, for the first time, that the NU encodes proprioceptive information, dynamically integrating it with vestibular signals while accounting for the head's orientation relative to the body. We propose that the synergistic integration of canal and otolith vestibular input with proprioceptive input in the NU enhances the encoding of self-motion in space to achieve robust head and body postural control.

RESULTS

NU Purkinje cell responses to vestibular stimulation

We recorded from 163 total Purkinje cells in the NU (Figure 1A). All Purkinje cells in our sample were sensitive to vestibular stimulation produced by applied whole-body translations and were insensitive to eye movements. We first examined each neuron's simple spike response to vestibular stimulation by applying whole-body translations along the anteroposterior and mediolateral axes (illustrated in Figure S1B). Figure 1A reveals the diversity in the vestibular responses that we observed among our population of Purkinje cells during anteroposterior translations. We show three example Purkinje cells that are representative of the primary response types observed in our population during vestibular stimulation. The first example Purkinje cell (Purkinje cell 1; left) linearly encoded vestibular information, displaying robust and opposite responses for posteriorly versus anteriorly directed translations. However, the majority of vestibular-sensitive Purkinje cells did not exhibit such linear responses. For instance, the middle and right of Figure 1A illustrate two other Purkinje cells. Purkinje cell 2 was excited by posteriorly but not anteriorly directed translations and thus demonstrated a half-wave rectifying response. Purkinje cell 3 exhibited a bidirectional excitation for applied anterior and posterior translation, resulting in a v-shaped response. Notably, we observed a similar heterogeneity in the responses of our population of Purkinje cells to mediolaterally directed translations (Figure S2), and group results of neuron response types can be seen in Figure S3A.

To quantify each Purkinje cell's sensitivity to vestibular stimulation, we performed least-squares linear regressions with three kinematic terms (head velocity, acceleration, and jerk) for movements in each direction (see STAR Methods). We included neurons that remained isolated across all three conditions (whole-body, body-under-head, and head-on-body) in the anteroposterior (n = 111) and/or mediolateral (n = 120) direction. The response sensitivities and phases to head motion were calculated from response gains for these three terms (see STAR Methods). Figure 1B illustrates these results, with histograms representing vestibular sensitivities and polar plots showing both the phase (vector angle) and sensitivity (vector magnitude) for each Purkinje cell. Overall, Purkinje cells showed considerable heterogeneity in their response dynamics. For stimulation in the anteroposterior direction, the responses of most neurons (53%) were in phase with linear acceleration, yet the responses of others were more aligned with velocity (33%) or jerk (15%) (Figure S3B, left). Likewise, for stimulation in the mediolateral direction, the responses of most neurons (52%) were in phase with linear acceleration, with the responses of others better aligned with linear velocity (31%) or jerk (18%) (Figure S3B, right).

We then classified the "preferred direction" of each Purkinje cell as the direction for each axis of stimulation that generated an increase in firing rate, or the larger increase in firing rate in the case of v-shaped cells. In response to anteroposterior translations, preferred directions were equally divided between both directions, with 58 Purkinje cells (52%) preferring posterior translations and the remainder preferring anterior translations. Likewise, in response to mediolateral translations, preferred directions were equally divided between both directions, with 62 Purkinje cells (52%) preferring ipsilateral translations and the remainder preferring contralateral translations.

NU Purkinje cell simple spike modulation by neck proprioceptive stimulation

We next examined whether and how vestibular-sensitive Purkinje cells respond to stimulation of neck proprioceptors. To assess sensitivities to comparable motion stimulation, the body was translated beneath an earth-stationary head using the same motion profile as vestibular stimulation (Figure 1A) to stretch the neck musculature. Figure 2A illustrates the responses of the same three Purkinje cells shown above in Figure 1A to body-under-head translations applied in the anteroposterior direction. Head-on-body movements made under natural conditions would stretch the neck muscles as if the head were moving in the opposite direction relative to the body (i.e., an anterior head movement would correspond to a posterior-directed stretch). Thus, to facilitate comparison with neuronal responses to applied vestibular stimulation, anterior translations of the body are shown with the opposite sign as in Figure 1. As observed for their responses to vestibular stimulation, Purkinje cells demonstrated considerable heterogeneity in their responses to proprioceptive stimulation. For example, while Purkinje cell 1 linearly encoded proprioceptive information, Purkinje cells 2 and 3 demonstrated half-wave rectified and v-shaped responses, respectively. We also observed a similar heterogeneity in the responses of our population of Purkinje cells to mediolaterally directed translations. Example cells are shown in Figure S4, and group results are shown in Figure S5A.

To quantify response dynamics, we then computed each Purkinje cell's sensitivity to proprioceptive stimulation using the same least-squares dynamic regression approach described above for the analysis of neural sensitivities to vestibular stimulation (see STAR Methods). Unexpectedly, our analysis revealed that the vast majority (90%–97%) of our Purkinje cell population demonstrated significant simple spike modulation during applied stimulation of neck proprioceptors (filled bars in Figure 2B). Figure 2B illustrates overall results, with histograms displaying vestibular sensitivities to proprioceptive stimulation and polar plots showing the phase and sensitivity of each Purkinje cell.

Please cite this article in press as: Mildren et al., Convergence of vestibular and proprioceptive signals in the cerebellar nodulus/uvula enhances the encoding of self-motion in primates, Current Biology (2024), https://doi.org/10.1016/j.cub.2024.11.063

CellPress

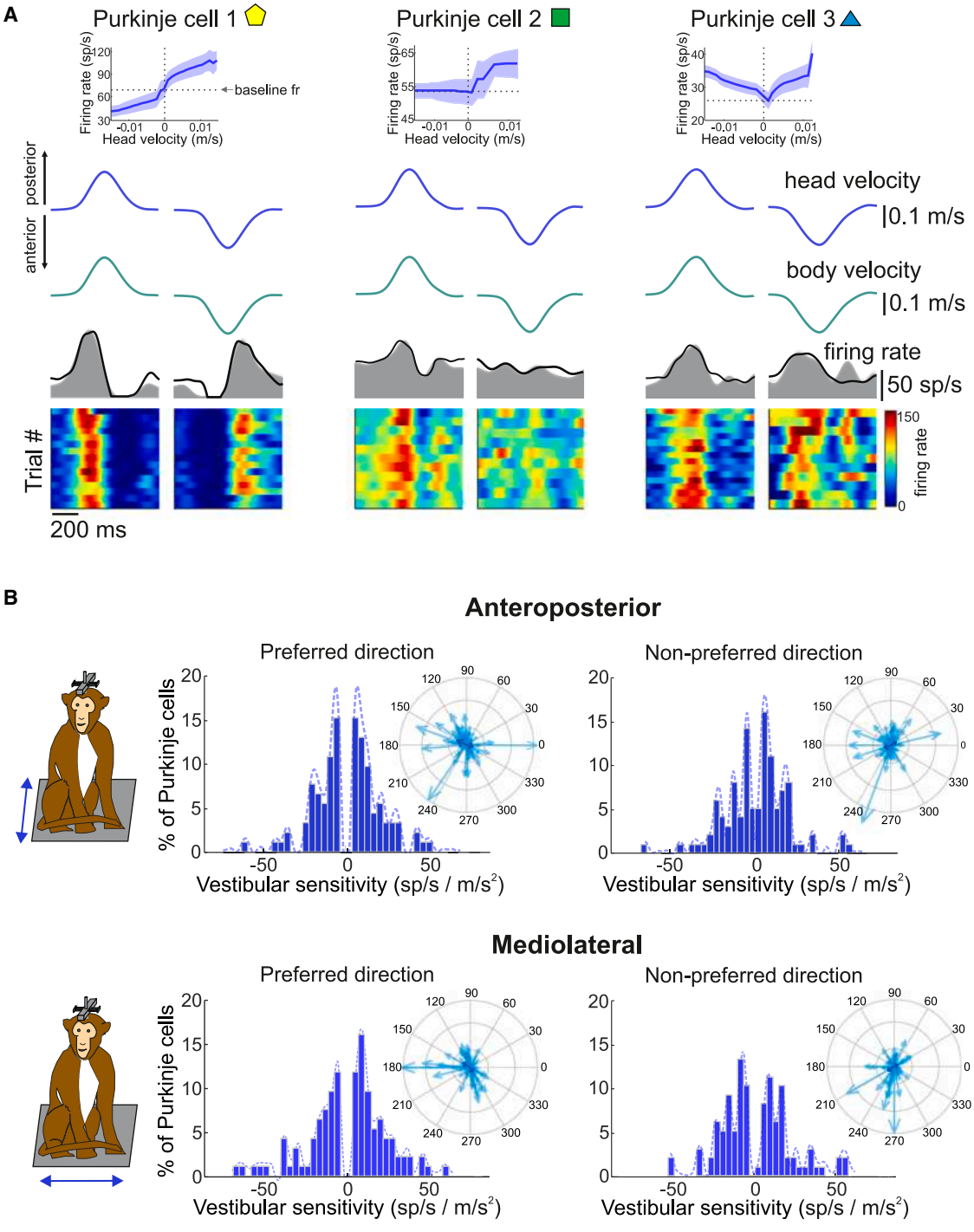

Figure 1. Responses of Purkinje cell simple spikes to vestibular stimulation

(A) We stimulated the vestibular system by applying passive whole-body translations in the anteroposterior and mediolateral directions. The simple spike firing rate responses are shown for three example NU Purkinje cells during anteroposterior translations. Head and body translation velocity are shown in the top two rows, and simple spike firing rate (gray shaded area) along with the linear estimation of the firing rate based on head motion (superimposed black trace) are shown in the bottom row. Heatmaps illustrate simple spike firing rates for each motion trial. Insets: simple spike firing rate as a function of head velocity in space.

(B) Distribution of Purkinje cell sensitivities to motion in the preferred (direction that generated the largest increase in firing rate) and non-preferred directions. Positive and negative values represent Purkinje cells with posterior versus anterior direction preferences (or ipsilateral versus contralateral for mediolateral translations). Insets: sensitivities (vector magnitude) and phases (vector angle) of each Purkinje cell's response to vestibular stimulation. Darker-filled arrows indicate population averages.

See also Figures S2 and S3.

Please cite this article in press as: Mildren et al., Convergence of vestibular and proprioceptive signals in the cerebellar nodulus/uvula enhances the encoding of self-motion in primates, Current Biology (2024), https://doi.org/10.1016/j.cub.2024.11.063

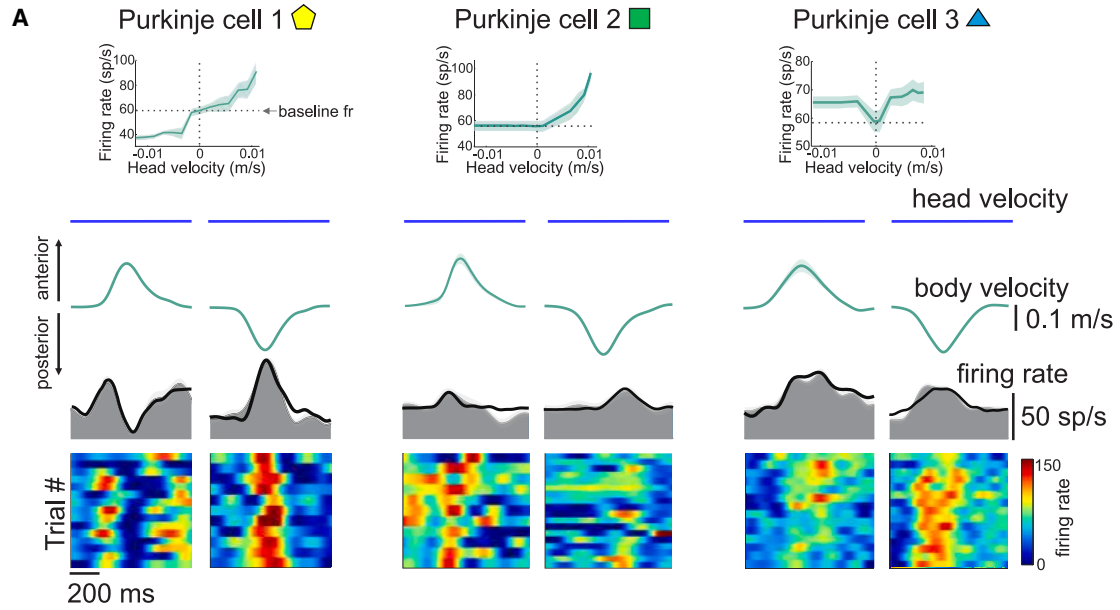

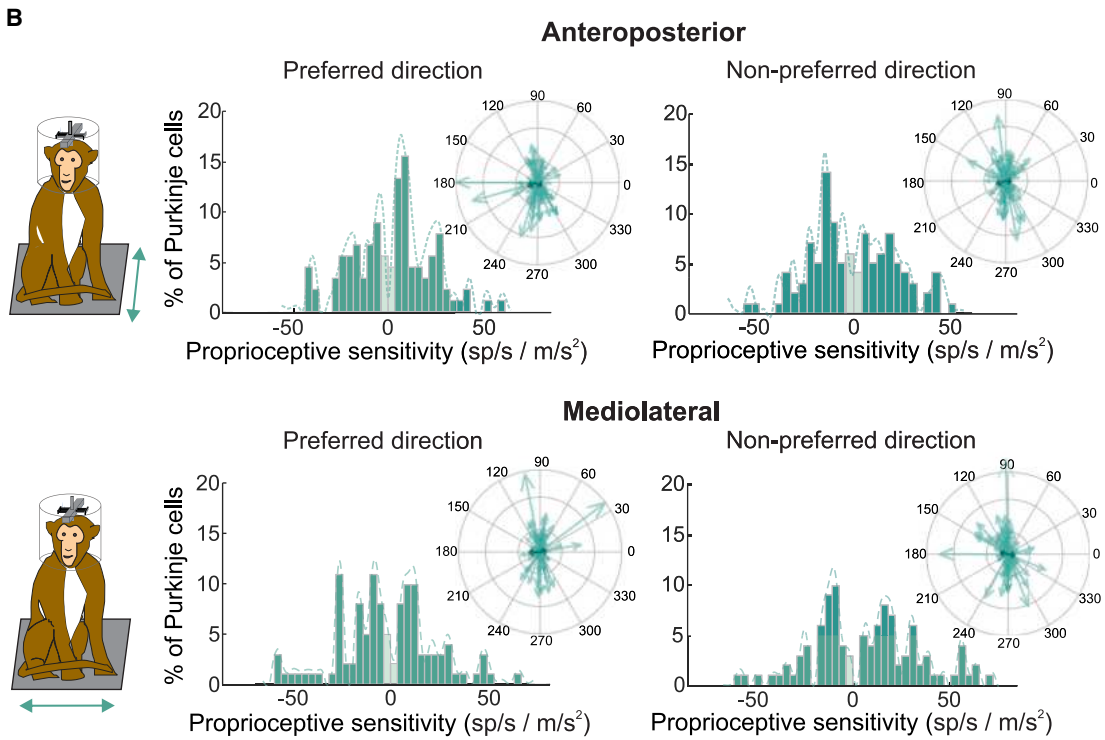

Figure 2. Responses of Purkinje cell simple spikes to neck proprioceptive stimulation

(A) We stimulated neck proprioceptors by applying passive translations of the body while holding the head stable in space. The simple spike firing rate responses are shown for the same three example NU Purkinje cells as shown in Figure 1. Head and body translation velocity are shown in the top two rows, and simple spike firing rate (gray shaded area) along with the linear estimation of the firing rate based on body motion (superimposed black trace) are shown in the bottom row. Heatmaps illustrate simple spike firing rates for each motion trial. Insets: simple spike firing rate as a function of body velocity in space.

(B) Distribution of Purkinje cell sensitivities to motion in the preferred and non-preferred directions. Positive and negative values represent Purkinje cells with anterior versus posterior body motion direction preferences (or contralateral versus ipsilateral for mediolateral translations), and open bars represent Purkinje cells with no significant response to proprioceptive stimulation. Insets: sensitivities (vector magnitude) and phases (vector angle) of each Purkinje cell's response to proprioceptive stimulation. Darker-filled arrows indicate population averages.

See also Figures S4 and S5.

Please cite this article in press as: Mildren et al., Convergence of vestibular and proprioceptive signals in the cerebellar nodulus/uvula enhances the encoding of self-motion in primates, Current Biology (2024), https://doi.org/10.1016/j.cub.2024.11.063

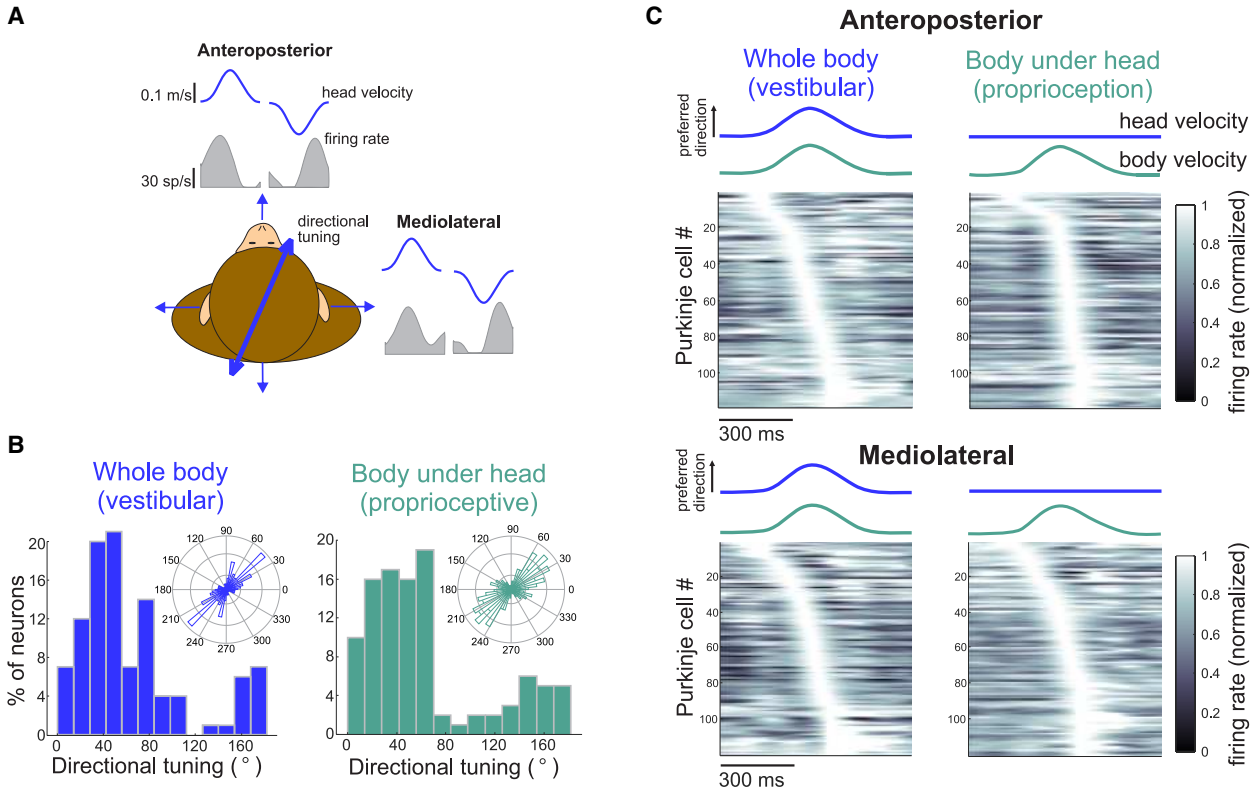

Figure 3. Directional tuning of Purkinje cell simple spike responses to vestibular and neck proprioceptive stimulation

(A) Illustration of one example Purkinje cell that showed comparable modulation to both anteroposterior and mediolateral translations, resulting in a directional tuning in between these cardinal axes.

(B) Distribution of Purkinje cell directional tunings for passive vestibular (left) and proprioceptive (right) stimulation. Insets: directional tuning distributions displayed in polar plots.

(C) Firing rate responses of each Purkinje cell to vestibular (whole-body translations; left) and neck proprioceptive (body-under-head translations; right) stimulation in both the anteroposterior and mediolateral directions. Firing rates were normalized to maximum firing rate, and Purkinje cell numbers were ordered by the location of their peak firing rate for illustrative purposes.

Moreover, as observed for their responses to vestibular stimulation, Purkinje cells demonstrated considerable heterogeneity in their response dynamics. Similar to vestibular stimulation, responses of most neurons to proprioceptive stimulation in the anteroposterior direction were in phase with linear acceleration (53%), while others were more aligned with velocity (41%) or jerk (6%) (Figure S5B, left). Likewise, for stimulation in the mediolateral direction, responses of most neurons (46%) were in phase with acceleration, with the responses of others better aligned with linear velocity (38%) or jerk (15%) (Figure S5B, right).

Similar to results for vestibular stimulation, we also found that preferred directions were equally divided between posterior and anterior directions for proprioceptive stimulation, with 57 Purkinje cells (51%) preferring posterior translations and the remainder preferring anterior translations. Likewise, in the mediolateral direction, 69 Purkinje cells (59%) preferred ipsilateral translations and the remainder preferred contralateral translations.

NU Purkinje cells show similar directional tuning to vestibular and neck proprioceptive stimulation

On the basis of each Purkinje cell's simple spike response to anteroposterior and mediolateral whole-body and body-under-head translations, we estimated its tuning direction for vestibular and proprioceptive stimulation, respectively (see STAR Methods) (n = 118 Purkinje cells for vestibular stimulation and n = 119 for proprioceptive stimulation). Figure 3A shows one example Purkinje cell's response to translations along the cardinal axes of motion, along with its estimated directional tuning, which fell along the oblique axis. Indeed, we found that overall, the tuning directions of our Purkinje cell population for vestibular stimulation tended to cluster around the oblique axes, which aligns more with the semicircular canals (Figure 3B, left). Such tuning for vestibular stimulation is consistent with prior reports[18] and has been suggested to facilitate the integration of canal and otolith information in computations that discriminate head tilts and translations. Interestingly, our analysis of proprioceptive responses likewise revealed that proprioceptive tuning tended to cluster around a similar axis (Figure 3B, right). Overall, the estimated tuning directions for vestibular versus proprioceptive stimulation were comparable (64.5° ± 47.8° versus 63.0° ± 50.5°, p = 0.8315).

Figure 3C illustrates the raw simple spike firing rate for each Purkinje cell during vestibular and proprioceptive stimulation along their preferred direction for both anteroposterior (top) and

Please cite this article in press as: Mildren et al., Convergence of vestibular and proprioceptive signals in the cerebellar nodulus/uvula enhances the encoding of self-motion in primates, Current Biology (2024), https://doi.org/10.1016/j.cub.2024.11.063

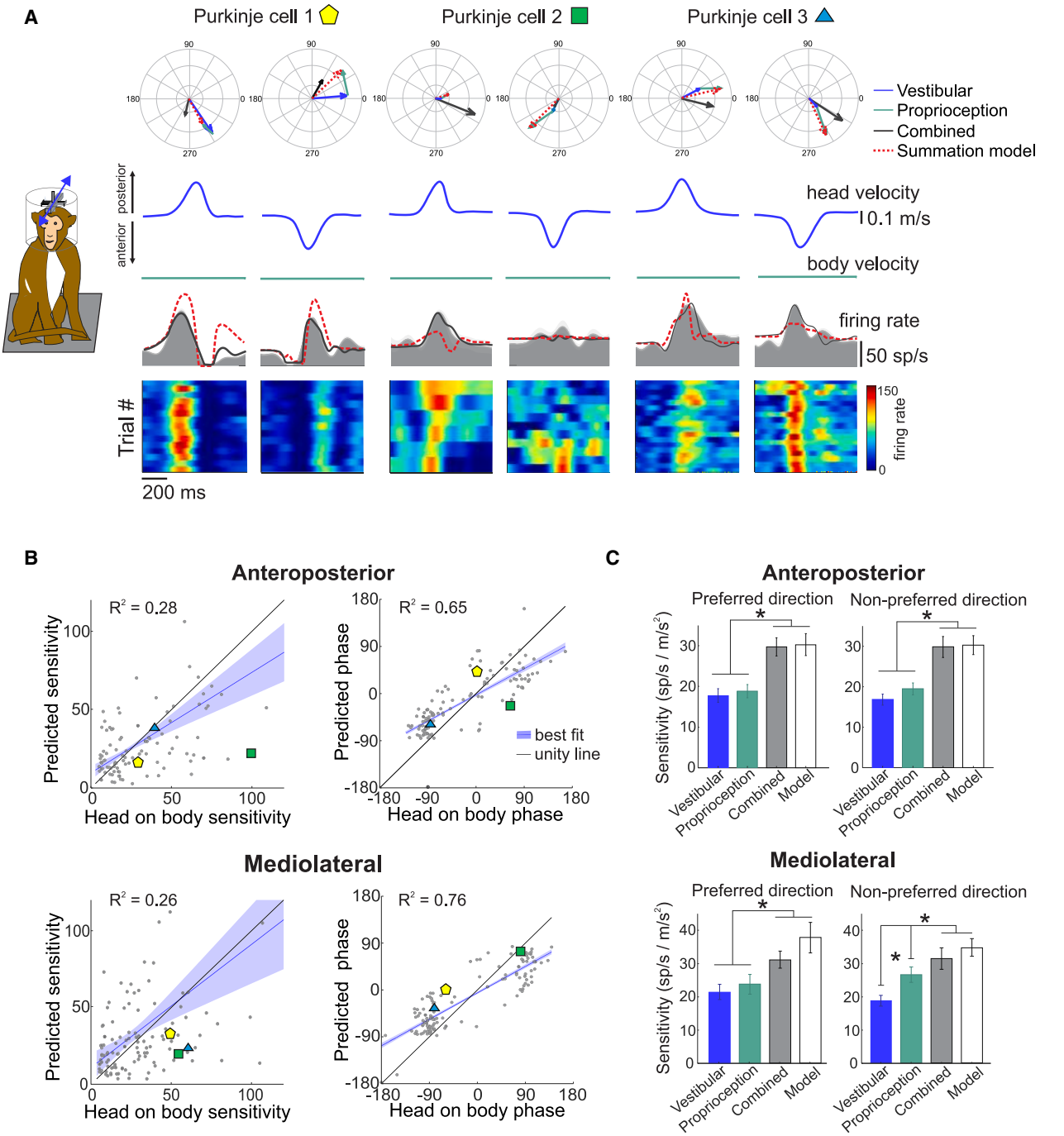

Figure 4. Responses of Purkinje cell simple spikes to combined vestibular and proprioceptive stimulation

(A) Combined vestibular and proprioceptive stimulation was generated by passively moving the head on the body. Responses are demonstrated for the same three example Purkinje cells shown in Figures 1 and 2, which can be identified in scatter plots below by their corresponding symbols. Polar plots (top row) demonstrate the sensitivity and phase of each Purkinje cell's response to passive vestibular, proprioceptive, and combined stimulation as well as the predicted sensitivity and phase from the summation model. The top two traces show head and body translation velocity, and the simple spike firing rate (gray shaded area) along with the linear estimation of the firing rate based on body motion (superimposed black trace) are shown in the bottom row. Heatmaps illustrate simple spike firing rates for each head motion trial.

(B) Estimated vs. predicted Purkinje cell sensitivities and phases to head-on-body translations in the preferred movement direction. The blue line and shading represent the linear fit and ±95% confidence interval.

(legend continued on next page)

Please cite this article in press as: Mildren et al., Convergence of vestibular and proprioceptive signals in the cerebellar nodulus/uvula enhances the encoding of self-motion in primates, Current Biology (2024), https://doi.org/10.1016/j.cub.2024.11.063

mediolateral (bottom) motion. Responses across the population are ordered by the location of each neuron's peak firing rate. These four plots illustrate how well nearly all recorded Purkinje cells are modulated by both vestibular and proprioceptive stimulation and in both translation directions, leading to the intermediate directional tuning observed in the histograms above. Furthermore, Figure 3C illustrates how the phases of the neural activity tile the phase of the stimulus profile, reflecting the heterogeneity of Purkinje cell response dynamics. Taken together, these findings reveal an exciting discovery, namely that both proprioceptive and vestibular encoding by NU Purkinje cells share a common directional tuning preference that aligns more closely with the canal axes rather than the cardinal axes (anteroposterior and mediolateral). This shared tuning underscores a significant integration mechanism that enhances our understanding of how sensory information is processed and utilized for precise motor control.

NU Purkinje cell responses to concurrent vestibular and proprioceptive stimulation

Our above findings have established that the majority of vestibular-sensitive Purkinje cells in our sample are also sensitive to neck proprioceptive stimulation. During natural movements, we move our head relative to our body, and as a result, the vestibular and proprioceptive systems are often stimulated concurrently. Accordingly, we next examined how NU Purkinje cells integrate these two streams of sensory input. To do this, we applied linear translations of the head relative to the body along the anteroposterior and mediolateral axes to simultaneously activate the vestibular and neck proprioceptive systems. Figure 4A illustrates the responses of the same 3 example Purkinje cells shown in Figures 1A and 2A above to applied passive head-on-body translations in the anteroposterior direction. The actual firing rate (gray) is plotted for each cell, and the firing rate prediction (red dashed traces) based on the vector summation of the Purkinje cell's response to vestibular and neck proprioceptive stimulation when presented independently—as described above for Figures 1 and 2—is superimposed. In addition, a linear estimation of firing rate based on head motion (solid dark gray trace) is included for comparison (see STAR Methods). The vectors within the polar plots (insets) represent the sensitivities and phases of the responses to vestibular stimulation alone (blue), proprioceptive stimulation alone (green), combined stimulation (black), as well as a model prediction based on a simple vector sum of vestibular and proprioceptive responses (red). Overall, the ability of the linear summation model to predict modulation for combined stimulation varied across Purkinje cells. Similar results were found for Purkinje cell responses to mediolateral head-on-body translations (Figure S6A).

Figures 4B and 4C summarize the data for our population of NU Purkinje cells across each of the three stimulation conditions for translations in the anteroposterior and mediolateral directions. Overall, response phases to combined stimulation were well matched to the linear summation model prediction (Figure 4B). While response sensitivities were not as well correlated, the mean fell along the unity line. Comparable results were found for our analyses of the non-preferred direction for both anteroposterior and mediolateral translations (Figure S6B). Group results demonstrated two important findings: first, on average the model prediction was similar to the sensitivity to combined stimulation (compare shaded gray versus open bars in Figure 4C). Second, Purkinje cell sensitivities to combined stimulation were enhanced relative to the sensitivities to vestibular or proprioceptive stimulation when presented alone ($p < 0.05$; compare blue and green bars with gray in Figure 4C). Overall, this indicates that vestibular and proprioceptive input tend to sum agonistically in the NU.

As mentioned earlier, generating appropriate vestibulospinal reflexes necessitates transforming vestibular information from a head-centered to a body-centered reference frame during self-motion. To further investigate the encoding of self-motion by NU Purkinje cells, we computed "head sensitivity" and "body sensitivity" ratios for each cell (Figure 5A; see STAR Methods). Theoretically, if a given neuron selectively encoded head motion in space, it would be assigned a head sensitivity ratio of 1 and a body sensitivity ratio of 0 (Figure 5, red star). This would occur if the neuron displayed comparable sensitivity to whole-body and head-on-body motion while being unresponsive to body-under-head motion. Conversely, if a given neuron selectively encoded only body motion in space, it would have a head sensitivity ratio of 0 and a body sensitivity ratio of −1 (Figure 5A, orange star). This would occur if the neuron displayed comparable sensitivity to whole-body and body-under-head motion while being unresponsive to head-on-body motion. Overall, compared with these theoretical neurons, we found that NU Purkinje cells in our sample demonstrated considerable heterogeneity in their sensitivity ratios, with the majority of NU Purkinje cells showing intermediate representations of head versus body motion for both anteroposterior and mediolateral translations in the preferred direction. Similar results were observed in the non-preferred directions (Figure S7A).

Next, to examine the transformation of vestibular self-motion information from head- to body-centered reference frames, we calculated a coding index (Figure 5B) that compares each Purkinje cell's sensitivity to head motion on the body to when only the body moved in space. We found that only a small proportion of Purkinje cells primarily encoded head (4% and 8%) or body (3% and 4%) motion in the preferred direction for anteroposterior and mediolateral translations, respectively (Figure 5B). Similar results were observed for motion in the non-preferred directions (Figure S7B). Together, these findings suggest the NU Purkinje cells integrate neck proprioceptive and vestibular signals to form an intermediate representation of dynamic head and body motion.

Purkinje cell vestibular responses are modulated by static head-on-body position

Previous studies in the rostral fastigial nucleus have revealed that the sensitivities of neurons that respond to both vestibular

(C) Bar graphs comparing sensitivities to vestibular, proprioceptive, combined stimulation, and summation model prediction for both the preferred and non-preferred directions for mediolateral and anteroposterior translations. Sensitivities were higher during combined stimulation compared with either vestibular or proprioceptive stimulation alone, and the linear summation model was not significantly different from the combined condition for all movement directions. See also Figure S6.

Please cite this article in press as: Mildren et al., Convergence of vestibular and proprioceptive signals in the cerebellar nodulus/uvula enhances the encoding of self-motion in primates, Current Biology (2024), https://doi.org/10.1016/j.cub.2024.11.063

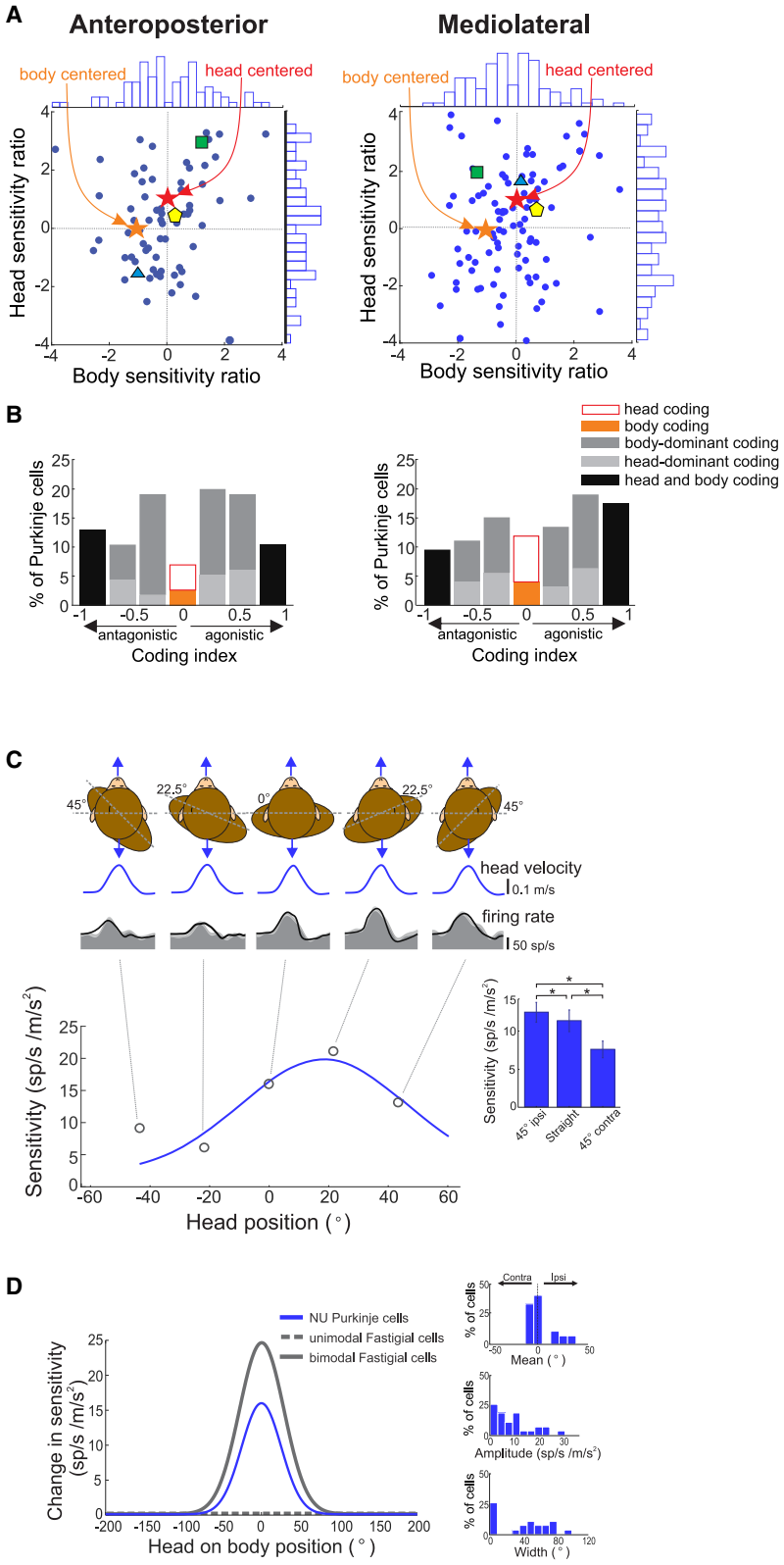

Figure 5. Encoding of dynamic head and body motion by NU Purkinje cell simple spikes and tuning of vestibular sensitivity to static head-on-body position

(A) Scatter plots show sensitivity ratios for head ($S_{vest+prop}/S_{vest}$) and body (S_{prop}/S_{vest}) motion for the preferred direction for anteroposterior and mediolateral translations. Histograms along the x and y axes display body- and head-sensitive ratio distributions. Sensitivity ratio results for the three example Purkinje cells can be identified in scatter plots below by their corresponding symbols. The orange star is positioned at values indicating pure body-centered coding, and the red star positioned at pure head-centered coding.

(B) Coding index distribution across Purkinje cells, illustrating the heterogeneity of head- versus body-dominant coding.

(C) The tuning curve of one example NU Purkinje cell assessed by applying whole-body translations in the naso-occipital direction with the head oriented at different positions on the body. Inset: bar graph comparing sensitivities of NU Purkinje cells (n = 27) between head orientations, where sensitivity was highest during ipsilateral and lowest during contralateral head-on-body positions.

(D) Average tuning curve obtained by aligning the means of all Purkinje cell's tuning curves, plotted with the tuning curve from fastigial neurons superimposed obtained from Shaikh et al.[30] Histograms (right) demonstrate the distribution of tuning means, amplitudes, and widths for NU Purkinje cells. Contra, contralateral; Ipsi, ipsilateral.

See also Figure S7.

Please cite this article in press as: Mildren et al., Convergence of vestibular and proprioceptive signals in the cerebellar nodulus/uvula enhances the encoding of self-motion in primates, Current Biology (2024), https://doi.org/10.1016/j.cub.2024.11.063

and neck proprioceptive input are modulated by changes in static head-on-body position.[30–32] This dynamic modulation of sensory responses based on postural signals (i.e., gain fields) aligns with common features in theoretical models of reference frame transformations.[33,34] Therefore, we explored the mechanism behind this tuning. Specifically, we investigated whether it is initially generated at the level of the NU Purkinje cells that target these nuclei. To test this hypothesis, we experimentally altered the static position of the head relative to the body and then examined NU Purkinje cell vestibular responses during whole-body translations applied along the same naso-occipital axis. For 27 Purkinje cells, we tested three static head positions (45° ipsilateral, 0°, and 45° contralateral). For a subset of 15 of these Purkinje cells, we tested two additional static head positions (22.5° ipsilateral and 22.5° contralateral).

Figure 5C illustrates a representative Purkinje cell that displayed stronger vestibular responses during ipsilateral static head-on-body positions. We found similar results across our population of Purkinje cells, with motion sensitivities higher when the head was rotated to the ipsilateral side (12.3 ± 6.7 sp/s/m/s^2) compared with the head being straight (11.2 ± 7.3 sp/s/m/s^2) and significantly lower when the head was rotated to the contralateral side (7.4 ± 5.7 sp/s/m/s^2) ($p < 0.05$) (Figure 5C, bar graph inset). To further quantify the tuning as a function of static head position, we fit Gaussian tuning curves to 15 of these Purkinje cells, as illustrated by the example in Figure 5C. The remaining 12 Purkinje cells were better fit by sigmoidal functions.[35] We calculated the mean, amplitude, and width of these tuning curves (Figure 5D, histograms) (there were no significant differences between the two fitting functions; $p < 0.05$). Notably, the mean of these tuning curves tended to be either near 0 (straight ahead) or toward the ipsilateral side, with no Purkinje cells in our sample showing a strong preference for contralateral head-on-body positions.

Finally, to compare the tuning observed in NU Purkinje cells with that observed in their target neurons, we compared our results to data previously described by Shaikh et al.[30] In comparison to bimodal fastigial nucleus neurons, NU Purkinje cells showed a similar width and lower amplitude tuning of sensitivity as a function of head-on-body position (Figure 5D). Thus, tuning to static head position becomes more pronounced in downstream target neurons relative to the output from the cerebellar cortex.

A population model consisting of a linear combination of Purkinje cell activities can predict the response of neurons in the vestibular and deep cerebellar nuclei

So far, our results have demonstrated that single bimodal Purkinje cells in the NU encode self-motion in a reference frame intermediate between head- and body-centered. In comparison, unimodal neurons in the vestibular and fastigial nuclei dynamically encode motion of the head (e.g., red star in Figure 5A), and bimodal neurons in the fastigial nucleus dynamically encode motion of the body (e.g., orange star in Figure 5A).[31,36] This indicates that the transformation from a head- to body-centered reference frame of self-motion would necessitate combining the activities of a population of Purkinje cells.

To test this hypothesis, we quantified the number of Purkinje cells required to produce responses of theoretical neurons that strictly encode either dynamic head or body motion using a simple linear model optimizing the weights of the activities of multiple NU Purkinje cells across stimulation conditions (whole-body, body-under-head, head-on-body), as illustrated in Figure 6A. Increasing the population size of Purkinje cells led to an increase in the goodness of fit for both anteroposterior (Figure 6B) and mediolateral motion (Figure S8B), as expected. Interestingly, we found that the weighted activity of ~30–40 NU Purkinje cells could generate the activity in either head or body encoding neurons that approximated their activity across conditions in the anteroposterior and mediolateral direction, with a smaller population necessary for head coding. As described above, we observed considerable heterogeneity across NU Purkinje cells regarding their dynamic sensitives to vestibular and proprioceptive stimulation. Thus, it is possible that particular Purkinje cells may have stronger weightings. However, we found a relatively continuous distribution of weightings across Purkinje cells, suggesting the response of target neurons was not dictated by a few Purkinje cells in the population model.

Head and body motion coding in NU versus anterior vermis Purkinje cells

Both the anterior and posterior vermis (NU) receive vestibular as well as proprioceptive input through either the external cuneate nucleus or central cervical nucleus[37–39] and project to the vestibular nuclei and medial deep cerebellar nucleus (fastigial).[40,41] However, there are some differences in their input and functions. The NU is the only cerebellar region that receives substantial direct input from primary vestibular afferents (illustrated in Figure S8A),[12,13,41] and lesions in this area produce severe impairments to trunk postural control in both humans[21] and monkeys.[25] Thus, the computations performed by the NU likely differ from the anterior vermis, which is involved in head- to body-centered reference frame transformations during horizontal rotations[42] and predicting the sensory feedback resulting from active self-motion.[43]

Thus, to contrast the computations performed by the anterior vermis versus the NU, we compared two measures: (1) the coding ratios for head versus body motion and (2) vestibular tuning as a function of static head-on-body position. First, to compare coding ratios for head versus body motion, we superimposed the data from Zobeiri and Cullen[42] and Figure 5A) onto the plots obtained in this study for NU Purkinje cells (Figure 5A, above). The resulting distributions of head versus body sensitivity ratios for anterior vermis and NU Purkinje cells are shown in Figures 7B and S9A, for stimulation in the anteroposterior and mediolateral directions, respectively. Interestingly, in comparison to anterior vermis Purkinje cells, a larger proportion of NU Purkinje cells had sensitivity ratios consistent with dynamic body/body-dominant coding (41%–54% versus 23%). Correspondingly, in comparison to anterior vermis Purkinje cells, a smaller proportion of NU Purkinje cells had sensitivity ratios consistent with head/head-dominant coding (21%–33% versus 70%). Second, to compare vestibular tuning as a function of static head-on-body position, we superimposed the average tuning curve computed in Zobeiri and Cullen[42] with that obtained in this study for NU Purkinje cells (Figure 5D, above), normalized to peak amplitude. Interestingly, as shown in Figure 7D, NU Purkinje cells

Please cite this article in press as: Mildren et al., Convergence of vestibular and proprioceptive signals in the cerebellar nodulus/uvula enhances the encoding of self-motion in primates, Current Biology (2024), https://doi.org/10.1016/j.cub.2024.11.063

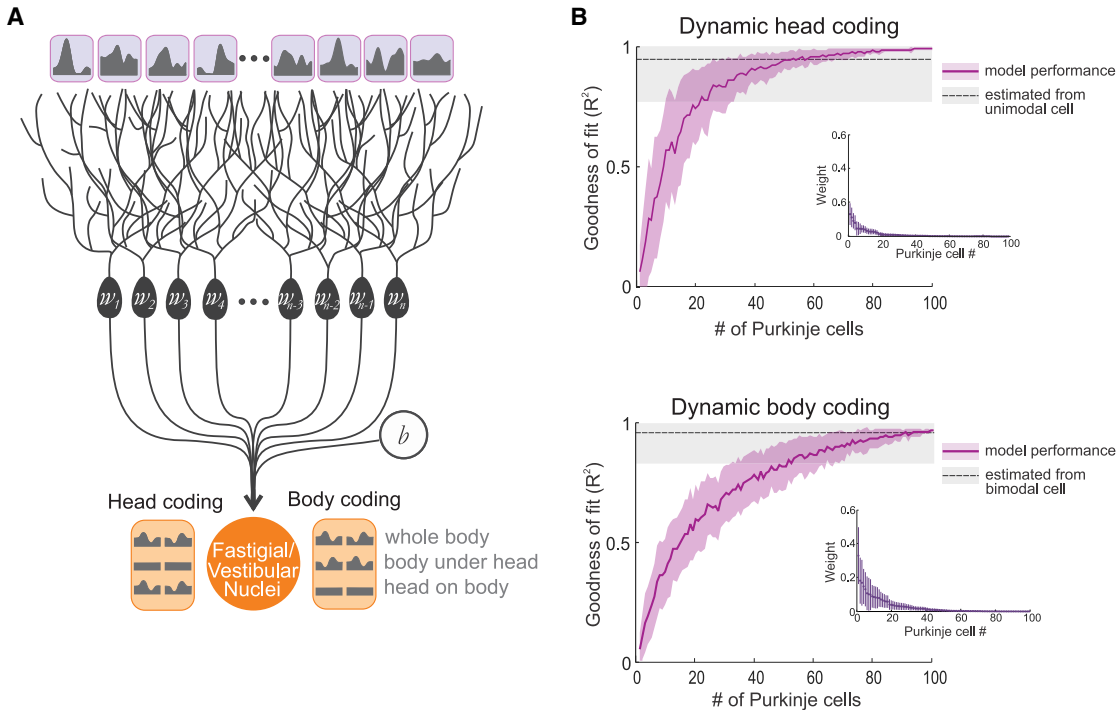

Figure 6. The integration of activities across Purkinje cells can explain the responses of head or body coding neurons across anteroposterior self-motion conditions

(A) Illustration of the linear model based on weighted activities across multiple Purkinje cells, which converge onto vestibular and fastigial nuclei neurons. Purkinje cell weights were optimized to provide the closest estimate of a purely head-coding (unimodal) or body-coding (bimodal) neuron's response during whole-body, body-under-head, and head-on-body conditions in the anteroposterior direction.

(B) Performance of the model for predicting dynamic head coding (upper) or body coding (lower) as the number of Purkinje cells included in the population increases. Purple line and shading represent the mean model fit and 95% confidence interval, and gray dashed line and shading represent the variability of fastigial nuclei neuron responses described by Brooks and Cullen.[31] Insets: the weightings of each Purkinje cell in the model sorted by their average weights. See also Figure S8.

demonstrated broader tuning compared with anterior vermis Purkinje cells (Figure 7D). Overall, these results suggest that in comparison to the anterior vermis, NU Purkinje cells demonstrate more robust coding of dynamic body motion.

DISCUSSION

Our results reveal, for the first time, that the NU integrates proprioceptive input synergistically with vestibular input to effectively enhance self-motion encoding in primates. Specifically, we found that the majority of Purkinje cells that responded to dynamic stimulation of the vestibular system also responded robustly to neck proprioceptive stimulation, and Purkinje cells aligned the directional tuning of their responses to both stimuli along the canal axes. Overall, the heterogeneity of Purkinje cell response dynamics enabled their population activity to generate head or body motion encoding in the downstream nuclei neurons that comprise the output of the cerebellum. Interestingly, when we altered the position of the head relative to the body, Purkinje cells modulated their response to the same otolith vestibular stimulation to account for the change in how the body is moving through space. Given that NU Purkinje cells converge onto vestibular and deep cerebellar nuclei neurons that are integral to motor, autonomic, and higher-order pathways,[40] we suggest the synergistic integration of canal and otolith along with proprioceptive input enhances the encoding of self-motion in space.

Purkinje cell vestibular responses are modulated by postural signals

It is well established that the rapid and early integration of proprioceptive cues with vestibular information is essential for maintaining posture during daily activities.[26–29,44,45] Notably, vestibulospinal reflexes make essential contributions to postural control, operating below perceptual self-motion thresholds.[46] However, since the vestibular organs are located within the head, the brain must account for the head's position relative to the body to accurately drive the vestibulospinal reflexes to control limb and axial musculature. There are many reasons to believe that the required integration of proprioceptive and vestibular information occurs within the cerebellum. For instance, transiently depressing activity in the human cerebellar vermis using transcranial magnetic stimulation impairs the transformation of vestibular-evoked responses based on head-on-body configuration.[47] Additionally, altering proprioceptive sensory input by turning the head or perturbing the sternocleidomastoid muscle influences cerebellar-evoked modulation of the motor cortex.[48] And furthermore, individual neurons in the fastigial

Please cite this article in press as: Mildren et al., Convergence of vestibular and proprioceptive signals in the cerebellar nodulus/uvula enhances the encoding of self-motion in primates, Current Biology (2024), https://doi.org/10.1016/j.cub.2024.11.063

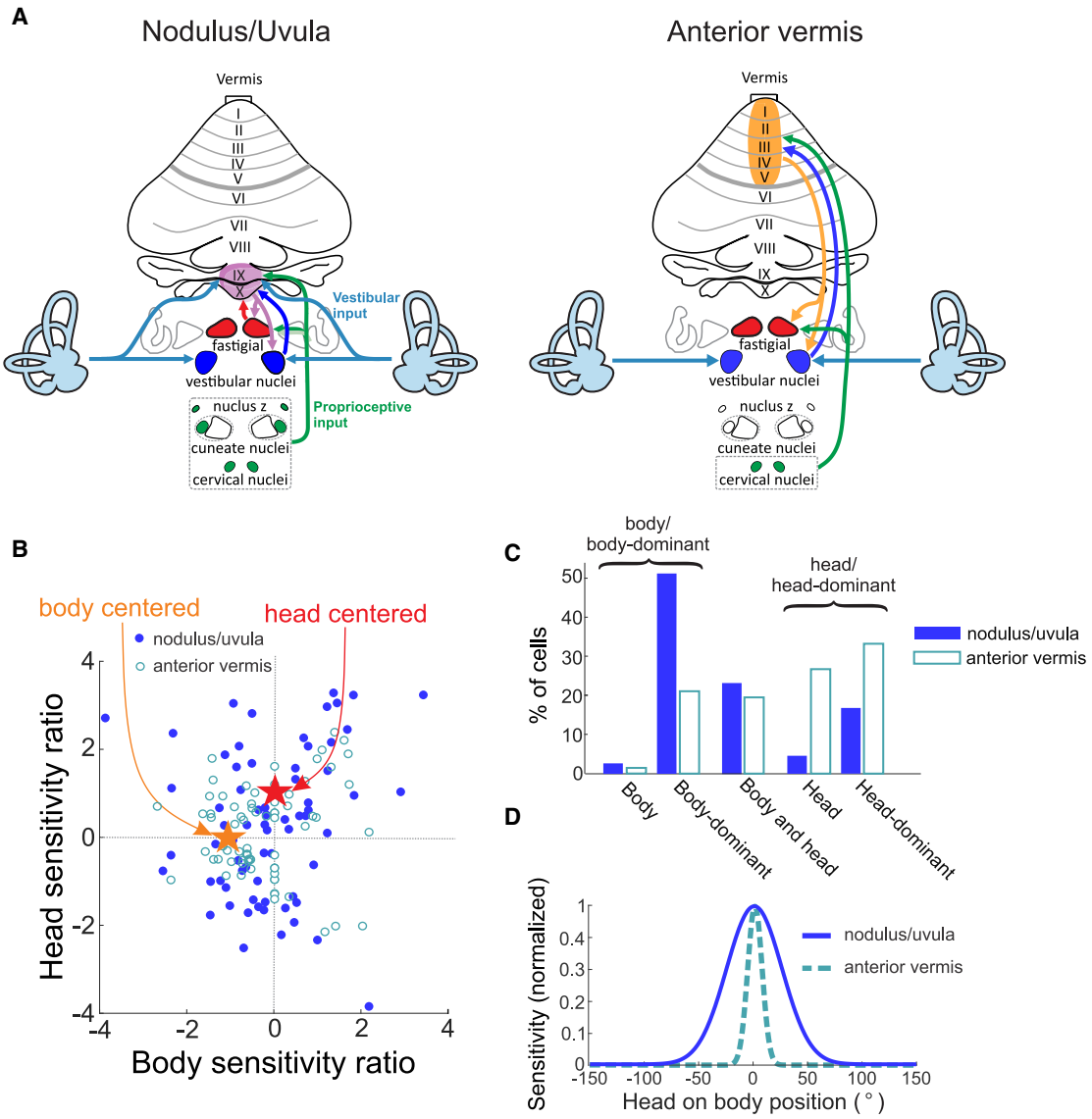

Figure 7. NU versus anterior vermis Purkinje cells differ in their sensory input as well as head and body motion encoding

(A) Illustration of the input and outputs of the NU (left) versus anterior vermis (right).

(B) Head and body sensitivity ratios for NU Purkinje cells during anteroposterior motion (filled circles), with anterior vermis Purkinje cells superimposed (open circles).

(C) Percentages of Purkinje cells in the NU versus anterior vermis that show head- or body-dominant coding, where a larger percentage of NU neurons show body-dominant coding.

(D) Comparison of the mean tuning curves of vestibular responses during different head-on-body positions in the NU (solid line) versus anterior vermis (dashed line).

See also Figure S9.

nucleus, a major downstream target of cerebellar Purkinje cells, integrate proprioceptive and vestibular information to encode body motion.[30–32,49]

The NU region of the posterior cerebellar vermis receives extensive direct projections from both vestibular afferents and the vestibular nuclei and, in turn, projects back to the vestibular nuclei as well as to the most medial of the deep cerebellar nuclei (fastigial nucleus) (reviewed in Laurens,[14] Cullen,[15] and Barmack and Pettorossi[41]). In humans, damage to the NU results in severe trunk ataxia, even while in a seated position.[21,22] Similarly, in monkeys, lesions of the NU result in frequent falls in all directions as well as head and trunk oscillations.[25] Based on these prior observations, we hypothesized that balance deficits following impaired NU function might arise, at least in part, from the disrupted integration of vestibular and proprioceptive signals. Indeed, in support of our hypothesis, our experiments revealed that more than 90% of vestibular-sensitive NU Purkinje cells dynamically encode proprioceptive information. Moreover,

Please cite this article in press as: Mildren et al., Convergence of vestibular and proprioceptive signals in the cerebellar nodulus/uvula enhances the encoding of self-motion in primates, Current Biology (2024), https://doi.org/10.1016/j.cub.2024.11.063

we found that the vestibular sensitivity of the majority of these same Purkinje cells displayed significant modulation as a function of static head-on-body position. It thus follows that NU lesions would disrupt normal vestibular-proprioceptive integration. This disruption would in turn alter the signals transmitted to the vestibular and deep cerebellar nuclei, resulting in the loss of accurate control over limb and axial musculature, thereby impairing the efficacy of vestibulospinal reflexes.

Mechanisms underlying dynamic coding of head and body motion

By quantifying the dynamics of NU Purkinje cells during passive proprioceptive stimulation induced by body-under-head linear motion, we further demonstrated that simple spike firing was primarily in phase with body acceleration. Additionally, most individual Purkinje cells displayed significant modulation to proprioceptive stimulation along both the anteroposterior and mediolateral directions. The estimated directional tuning across Purkinje cells clustered around the oblique rather than strictly anteroposterior or mediolateral directions. Moreover, we found that passive vestibular stimulation induced by whole-body translations elicited simple spike firing that was in phase with acceleration, and that the estimated directional tuning mirrored that observed for proprioceptive stimulation. One limitation is that our directional tuning was calculated from responses to stimulation applied in only two directions; however, our findings are consistent with previous characterizations of NU Purkinje cell responses to passive vestibular stimulation.[19,50] Taken together, our present findings reveal that the dynamic coding of head and body motion is well matched in the NU. We speculate that the alignment of this directional tuning along the orientation of the semicircular canals may facilitate the integration of proprioceptive with otolith and canal input.

Overall, our results show that, as a population, NU Purkinje cells respond equally strongly to proprioceptive and vestibular stimulation during linear self-motion. This raises the question: What is the source of this robust proprioceptive input to the NU? Likely sources include the external cuneate nucleus, central cervical nucleus, and nucleus Z, all of which encode proprioceptive information[51–53] and send projections to the NU.[10,37,39,40] While the central cervical nucleus relays proprioceptive information from the neck,[52] which was the focus of our study, the external cuneate nucleus and nucleus z provide proprioceptive information from the upper and lower limbs.[51,53] Thus, the circuitry of the NU is consistent with a role in integrating vestibular and proprioceptive information to generate appropriate postural responses in neck as well as axial musculature. Our present findings establish that NU Purkinje cells combine this neck proprioceptive input with input from primary vestibular afferents and the vestibular nuclei to shape simple spiking activity. Future research should examine whether and how limb proprioceptive feedback is integrated with vestibular signals in the NU.

This then leads to the follow-up question: what is the purpose of vestibular and proprioceptive integration at the level of NU Purkinje cells? On the one hand, our findings support the proposal that a primary function of this integration is to signal head motion for postural control of the head-neck system, specifically through the vestibulocollic reflex (VCR). We found that proprioceptive input combines agonistically with vestibular input to enhance the simple spike response to head motion—a computation that would be beneficial to support the VCR. This perspective aligns with a recent study by Buron et al.,[54] which found that the tuning properties of NU cells are consistent with head-centered coding of otolith signals during translations. On the other hand, our results also demonstrate that a population of NU Purkinje cells can compute dynamic body motion, and most individual cells show significant changes in sensitivity with static head-on-body position (i.e., gain fields). Similarly, Buron et al.[54] reported that a significant percentage of NU Purkinje cells exhibit gain fields. Together, these findings provide insight into the computations performed by the NU, underlying previous observations that lesions cause severe impairments in trunk postural control,[25] and thus implicate the NU in regulating postural control of both the body and the head-neck system. Future studies should investigate how NU Purkinje cells respond to dynamic vestibular and proprioceptive stimulation that reflect changes in head and body orientation relative to gravity.

Multisensory integration across the cerebellar vermis

Our present findings demonstrate that proprioceptive information is integrated into NU Purkinje cell simple spike activity. Surprisingly, prior literature includes only a single qualitative report indicating that NU Purkinje cells respond to dynamic proprioceptive stimulation, which was generated by pressing on neck muscles.[55] Thus, similar to the cerebellar anterior vermis, our data indicate that the NU of the posterior vermis is a key region in which Purkinje cells integrate vestibular and neck proprioceptive inputs. Integrated vestibular and proprioceptive information could also be relayed to the vermis via feedback from the target nuclei (vestibular and fastigial nuclei). In species including cats,[56] squirrel, and cynomolgus macaque monkeys,[57,58] vestibular nuclei neurons have been found to encode proprioceptive information; however, this is not the case in rhesus monkeys with an intact vestibular system.[59] However, the rostral fastigial nucleus does receive direct proprioceptive input from the central cervical nucleus, and neurons in this structure do respond to passively applied vestibular as well as proprioceptive stimulation.[31] Thus, given that the fastigial nucleus sends projections back to the NU, the NU effectively receives integrated input from this structure. Anterior vermis Purkinje cells likewise exhibit heterogeneity in their encoding of vestibular and proprioceptive information.[42] However, it is notable that, unlike the enhancement observed here for NU Purkinje cells during coincident vestibular and proprioceptive stimulation due to their agonistic tuning, the relative tuning of these two sensory inputs is generally antagonistic in anterior vermis Purkinje cells (e.g., Figures 3A and 3B[42]).

Both anterior vermis and NU Purkinje cells project strongly to the vestibular nuclei, forming essential pathways for head-neck and body postural control as well as self-motion perception. Additionally, while Purkinje cells from both regions project to the fastigial nucleus, there is only partial overlap in their target regions[60] and limited convergence of Purkinje cells from the anterior and posterior lobules onto the same target neuron.[61] Notably, anterior vermis Purkinje cells primarily project to rostral fastigial nucleus regions involved in postural control,[58] while NU Purkinje cells predominantly target a more ventral region.[60,62–64] This ventral region sends widespread connections to cortical and

subcortical areas related to attention, arousal, autonomic regulation, spatial navigation, memory, and motor control.[60,65–67] Thus, both cerebellar vermis regions send unique self-motion signals to distinct pathways involved in postural and autonomic regulation, and higher-order functions. Prior work has focused on the NU's role in encoding head tilt versus translation.[16,18–20,68] Importantly, our findings reveal the integration of proprioceptive signals with canal and otolith input in the NU, offering new insights into neural computations performed by the NU and the impact of lesions on balance.[21,22,25] We conclude that the NU integrates sensory input from the vestibular and proprioceptive systems, adjusting for gravity to maintain balance and stabilize posture.

RESOURCE AVAILABILITY

Lead contact

Requests for further information should be directed to the lead contact, Kathleen Cullen (kathleen.cullen@jh.edu).

Materials availability

This study did not generate new reagents.

Data and code availability

- Data have been deposited at figshare and are publicly available as of the date of publication at https://doi.org/10.6084/m9.figshare.27327750.v1.
- This paper does not report original code.
- Any additional information required to reanalyze the data reported in this paper is available from the lead contact upon request.

ACKNOWLEDGMENTS

We thank D. Roberts for technical assistance and Dr. T. Harris for providing the prototype high-density read-write electrodes along with technical expertise. We thank Skyler Thomas for his insight into analysis and all Cullen lab members for their detailed review of the manuscript and figures. This work was supported by funding from the National Institute on Deafness and Other Communication Disorders (R01-DC002390 and R01-DC018061) (K.E.C.) as well as a Natural Sciences and Engineering Postdoctoral Fellowship and Kavli Neuroscience Discovery Institute Distinguished Postdoctoral Fellowship (R.L.M.).

AUTHOR CONTRIBUTIONS

R.L.M. designed and conducted all experiments, analyzed the data, and wrote the manuscript. L.J.G. assisted with data collection and analysis and provided revisions to the manuscript. K.E.C. designed the experiments, supervised the project, and wrote the manuscript.

DECLARATION OF INTERESTS

The authors declare no competing interests.

STAR★METHODS

Detailed methods are provided in the online version of this paper and include the following:

- KEY RESOURCES TABLE
- EXPERIMENTAL MODEL AND STUDY PARTICIPANT DETAILS
- METHOD DETAILS
  - Surgical procedures
  - Experimental procedures
  - Data acquisition
- QUANTIFICATION AND STATISTICAL ANALYSIS

SUPPLEMENTAL INFORMATION

Supplemental information can be found online at https://doi.org/10.1016/j.cub.2024.11.063.

Received: September 25, 2024
Revised: October 31, 2024
Accepted: November 26, 2024
Published: January 9, 2025

REFERENCES

1. Liu, Z., Hildebrand, D.G.C., Morgan, J.L., Jia, Y., Slimmon, N., and Bagnall, M.W. (2022). Organization of the gravity-sensing system in zebrafish. Nat. Commun. *13*, 5060. https://doi.org/10.1038/s41467-022-32824-w.
2. Lackner, J.R., and DiZio, P. (2005). Vestibular, proprioceptive, and haptic contributions to spatial orientation. Annu. Rev. Psychol. *56*, 115–147. https://doi.org/10.1146/annurev.psych.55.090902.142023.
3. Keshner, E.A. (2003). Head-trunk coordination during linear anterior-posterior translations. J. Neurophysiol. *89*, 1891–1901. https://doi.org/10.1152/jn.00836.2001.
4. Barmack, N.H. (2003). Central vestibular system: vestibular nuclei and posterior cerebellum. Brain Res. Bull. *60*, 511–541. https://doi.org/10.1016/s0361-9230(03)00055-8.
5. Naito, Y., Newman, A., Lee, W.S., Beykirch, K., and Honrubia, V. (1995). Projections of the individual vestibular end-organs in the brain stem of the squirrel monkey. Hear. Res. *87*, 141–155. https://doi.org/10.1016/0378-5955(95)00085-i.
6. Newlands, S.D., Vrabec, J.T., Purcell, I.M., Stewart, C.M., Zimmerman, B.E., and Perachio, A.A. (2003). Central projections of the saccular and utricular nerves in macaques. J. Comp. Neurol. *466*, 31–47. https://doi.org/10.1002/cne.10876.
7. Brodal, A., and Torvik, A. (1957). Uber den Ursprung der sekundären vestibulo-cerebellaren Fasern bei der Katze; eine experimentell-anatomische Studie [The origin of secondary vestibulo-cerebellar fibers in cats; an experimental anatomical study]. Arch. Psychiatr. Nervenkr. Z. Gesamte Neurol. Psychiatr. *195*, 550–567. https://doi.org/10.1007/BF00343130.
8. Kotchabhakdi, N., and Walberg, F. (1978). Cerebellar afferent projections from the vestibular nuclei in the cat: an experimental study with the method of retrograde axonal transport of horseradish peroxidase. Exp. Brain Res. *31*, 591–604. https://doi.org/10.1007/BF00239814.
9. Yamamoto, M. (1979). Topographical representation in rabbit cerebellar flocculus for various afferent inputs from the brainstem investigated by means of retrograde axonal transport of horseradish peroxidase. Neurosci. Lett. *12*, 29–34. https://doi.org/10.1016/0304-3940(79)91475-7.
10. Brodal, A., and Brodal, P. (1985). Observations on the secondary vestibulocerebellar projections in the macaque monkey. Exp. Brain Res. *58*, 62–74. https://doi.org/10.1007/BF00238954.
11. Thunnissen, I.E., Epema, A.H., and Gerrits, N.M. (1989). Secondary vestibulocerebellar mossy fiber projection to the caudal vermis in the rabbit. J. Comp. Neurol. *290*, 262–277. https://doi.org/10.1002/cne.902900207.
12. Carleton, S.C., and Carpenter, M.B. (1984). Distribution of primary vestibular fibers in the brainstem and cerebellum of the monkey. Brain Res. *294*, 281–298. https://doi.org/10.1016/0006-8993(84)91040-0.
13. Maklad, A., and Fritzsch, B. (2003). Development of vestibular afferent projections into the hindbrain and their central targets. Brain Res. Bull. *60*, 497–510. https://doi.org/10.1016/s0361-9230(03)00054-6.
14. Laurens, J. (2022). The otolith vermis: A systems neuroscience theory of the Nodulus and uvula. Front. Syst. Neurosci. *16*, 886284. https://doi.org/10.3389/fnsys.2022.886284.
15. Cullen, K.E. (2023). Internal models of self-motion: neural computations by the vestibular cerebellum. Trends Neurosci. *46*, 986–1002. https://doi.org/10.1016/j.tins.2023.08.009.

16. Angelaki, D.E., and Hess, B.J. (1995). Inertial representation of angular motion in the vestibular system of rhesus monkeys. II. Otolith-controlled transformation that depends on an intact cerebellar nodulus. J. Neurophysiol. *73*, 1729–1751. https://doi.org/10.1152/jn.1995.73.5.1729.

17. Cohen, B., Wearne, S., Dai, M., and Raphan, T. (1999). Spatial orientation of the angular vestibulo-ocular reflex. J. Vestib. Res. *9*, 163–172. https://doi.org/10.3233/VES-1999-9303.

18. Yakusheva, T., Blazquez, P.M., and Angelaki, D.E. (2008). Frequency-selective coding of translation and tilt in macaque cerebellar nodulus and uvula. J. Neurosci. *28*, 9997–10009. https://doi.org/10.1523/JNEUROSCI.2232-08.2008.

19. Yakusheva, T., Blazquez, P.M., and Angelaki, D.E. (2010). Relationship between complex and simple spike activity in macaque caudal vermis during three-dimensional vestibular stimulation. J. Neurosci. *30*, 8111–8126. https://doi.org/10.1523/JNEUROSCI.5779-09.2010.

20. Laurens, J., Meng, H., and Angelaki, D.E. (2013). Computation of linear acceleration through an internal model in the macaque cerebellum. Nat. Neurosci. *16*, 1701–1708. https://doi.org/10.1038/nn.3530.

21. Mauritz, K.H., Dichgans, J., and Hufschmidt, A. (1979). Quantitative analysis of stance in late cortical cerebellar atrophy of the anterior lobe and other forms of cerebellar ataxia. Brain *102*, 461–482. https://doi.org/10.1093/brain/102.3.461.

22. Bailey, P., and Cushing, H. (1925). Medulloblastoma cerebelli: a common type of midcerebellar glioma of childhood. Arch. Neurol. Psychiatry, Chicago *14*, 192–223.

23. Diener, H.C., Dichgans, J., Bacher, M., and Guschlbauer, B. (1984). Characteristic alterations of long-loop "reflexes" in patients with Friedreich's disease and late atrophy of the cerebellar anterior lobe. J. Neurol. Neurosurg. Psychiatry *47*, 679–685. https://doi.org/10.1136/jnnp.47.7.679.

24. Ye, B.S., Kim, Y.D., Nam, H.S., Lee, H.S., Nam, C.M., and Heo, J.H. (2010). Clinical manifestations of cerebellar infarction according to specific lobular involvement. Cerebellum *9*, 571–579. https://doi.org/10.1007/s12311-010-0200-y.

25. Dow, R.S. (1938). Effect of lesions in the vestibular part of the cerebellum in primates. Arch. Neurol. Psychiatry *40*, 500–520. https://doi.org/10.1001/archneurpsyc.1938.02270090094005.

26. Tokita, T., Ito, Y., and Takagi, K. (1989). Modulation by head and trunk positions of the vestibulo-spinal reflexes evoked by galvanic stimulation of the labyrinth. Observations by labyrinthine evoked EMG. Acta Otolaryngol. *107*, 327–332. https://doi.org/10.3109/00016488909127516.

27. Kennedy, P.M., and Inglis, J.T. (2002). Interaction effects of galvanic vestibular stimulation and head position on the soleus H reflex in humans. Clin. Neurophysiol. *113*, 1709–1714. https://doi.org/10.1016/s1388-2457(02)00238-9.

28. Nashner, L.M., and Wolfson, P. (1974). Influence of head position and proprioceptive cues on short latency postural reflexes evoked by galvanic stimulation of the human labyrinth. Brain Res. *67*, 255–268. https://doi.org/10.1016/0006-8993(74)90276-5.

29. Dalton, B.H., Rasman, B.G., Inglis, J.T., and Blouin, J.S. (2017). The internal representation of head orientation differs for conscious perception and balance control. J. Physiol. *595*, 2731–2749. https://doi.org/10.1113/JP272998.

30. Shaikh, A.G., Meng, H., and Angelaki, D.E. (2004). Multiple reference frames for motion in the primate cerebellum. J. Neurosci. *24*, 4491–4497. https://doi.org/10.1523/JNEUROSCI.0109-04.2004.

31. Brooks, J.X., and Cullen, K.E. (2009). Multimodal integration in rostral fastigial nucleus provides an estimate of body movement. J. Neurosci. *29*, 10499–10511. https://doi.org/10.1523/JNEUROSCI.1937-09.2009.

32. Kleine, J.F., Guan, Y., Kipiani, E., Glonti, L., Hoshi, M., and Büttner, U. (2004). Trunk position influences vestibular responses of fastigial nucleus neurons in the alert monkey. J. Neurophysiol. *91*, 2090–2100. https://doi.org/10.1152/jn.00849.2003.

33. Pouget, A., and Snyder, L.H. (2000). Computational approaches to sensorimotor transformations. Nat. Neurosci. *3*, 1192–1198. https://doi.org/10.1038/81469.

34. Salinas, E., and Abbott, L.F. (2001). Coordinate transformations in the visual system: how to generate gain fields and what to compute with them. Prog. Brain Res. *130*, 175–190. https://doi.org/10.1016/s0079-6123(01)30012-2.

35. Zhang, T., Heuer, H.W., and Britten, K.H. (2004). Parietal area VIP neuronal responses to heading stimuli are encoded in head-centered coordinates. Neuron *42*, 993–1001. https://doi.org/10.1016/j.neuron.2004.06.008.

36. Carriot, J., Brooks, J.X., and Cullen, K.E. (2013). Multimodal integration of self-motion cues in the vestibular system: active versus passive translations. J. Neurosci. *33*, 19555–19566. https://doi.org/10.1523/JNEUROSCI.3051-13.2013.

37. Matsushita, M., and Tanami, T. (1987). Spinocerebellar projections from the central cervical nucleus in the cat, as studied by anterograde transport of wheat germ agglutinin-horseradish peroxidase. J. Comp. Neurol. *266*, 376–397. https://doi.org/10.1002/cne.902660306.

38. Matsushita, M., and Wang, C.L. (1987). Projection pattern of vestibulocerebellar fibers in the anterior vermis of the cat: an anterograde wheat germ agglutinin-horseradish peroxidase study. Neurosci. Lett. *74*, 25–30. https://doi.org/10.1016/0304-3940(87)90045-0.

39. Jasmin, L., and Courville, J. (1987). Distribution of external cuneate nucleus afferents to the cerebellum: I. Notes on the projections from the main cuneate and other adjacent nuclei. An experimental study with radioactive tracers in the cat. J. Comp. Neurol. *261*, 481–496. https://doi.org/10.1002/cne.902610403.

40. Voogd, J., Gerrits, N.M., and Ruigrok, T.J. (1996). Organization of the vestibulocerebellum. Ann. N. Y. Acad. Sci. *781*, 553–579. https://doi.org/10.1111/j.1749-6632.1996.tb15728.x.

41. Barmack, N.H., and Pettorossi, V.E. (2021). Adaptive balance in posterior cerebellum. Front. Neurol. *12*, 635259. https://doi.org/10.3389/fneur.2021.635259.

42. Zobeiri, O.A., and Cullen, K.E. (2022). Distinct representations of body and head motion are dynamically encoded by Purkinje cell populations in the macaque cerebellum. eLife *11*, e75018. https://doi.org/10.7554/eLife.75018.

43. Zobeiri, O.A., and Cullen, K.E. (2024). Cerebellar Purkinje cells in male macaques combine sensory and motor information to predict the sensory consequences of active self-motion. Nat. Commun. *15*, 4003. https://doi.org/10.1038/s41467-024-48376-0.

44. Hlavacka, F., and Njiokiktjien, C. (1985). Postural responses evoked by sinusoidal galvanic stimulation of the labyrinth. Influence of head position. Acta Otolaryngol. *99*, 107–112. https://doi.org/10.3109/00016488509119152.

45. Fransson, P.A., Karlberg, M., Sterner, T., and Magnusson, M. (2000). Direction of galvanically-induced vestibulo-postural responses during active and passive neck torsion. Acta Otolaryngol. *120*, 500–503. https://doi.org/10.1080/000164800750045992.

46. Tisserand, R., Rasman, B.G., Omerovic, N., Peters, R.M., Forbes, P.A., and Blouin, J.S. (2022). Unperceived motor actions of the balance system interfere with the causal attribution of self-motion. PNAS Nexus *1*, pgac174. https://doi.org/10.1093/pnasnexus/pgac174.

47. Lam, C.K., Tokuno, C.D., Staines, W.R., and Bent, L.R. (2016). The direction of the postural response to a vestibular perturbation is mediated by the cerebellar vermis. Exp. Brain Res. *234*, 3689–3697. https://doi.org/10.1007/s00221-016-4766-6.

48. Popa, T., Hubsch, C., James, P., Richard, A., Russo, M., Pradeep, S., Krishan, S., Roze, E., Meunier, S., and Kishore, A. (2018). Abnormal cerebellar processing of the neck proprioceptive information drives dysfunctions in cervical dystonia. Sci. Rep. *8*, 2263. https://doi.org/10.1038/s41598-018-20510-1.

49. Martin, C.Z.B., Brooks, J.X., and Green, A.M. (2018). Role of rostral fastigial neurons in encoding a body-centered representation of translation in

three dimensions. J. Neurosci. *38*, 3584–3602. https://doi.org/10.1523/JNEUROSCI.2116-17.2018.

50. Laurens, J., and Angelaki, D.E. (2020). Simple spike dynamics of Purkinje cells in the macaque vestibulo-cerebellum during passive whole-body self-motion. Proc. Natl. Acad. Sci. USA *117*, 3232–3238. https://doi.org/10.1073/pnas.1915873117.
51. Witham, C.L., and Baker, S.N. (2011). Modulation and transmission of peripheral inputs in monkey cuneate and external cuneate nuclei. J. Neurophysiol. *106*, 2764–2775. https://doi.org/10.1152/jn.00449.2011.
52. Hirai, N., Hongo, T., Sasaki, S., Yamashita, M., and Yoshida, K. (1984). Neck muscle afferent input to spinocerebellar tract cells of the central cervical nucleus in the cat. Exp. Brain Res. *55*, 286–300. https://doi.org/10.1007/BF00237279.
53. Low, J.S., Mantle-St John, L.A., and Tracey, D.J. (1986). Nucleus z in the rat: spinal afferents from collaterals of dorsal spinocerebellar tract neurons. J. Comp. Neurol. *243*, 510–526. https://doi.org/10.1002/cne.902430406.
54. Buron, F.M., Brooks, C.Z., Green, J.X., and A. M.. (2023). Reference frames for encoding of translation and tilt in the caudal cerebellar vermis. Preprint at bioRxiv. https://doi.org/10.1101/2023.09.09.556993.
55. Sheliga, B.M., Yakushin, S.B., Silvers, A., Raphan, T., and Cohen, B. (1999). Control of spatial orientation of the angular vestibulo-ocular reflex by the nodulus and uvula of the vestibulocerebellum. Ann. N. Y. Acad. Sci. *871*, 94–122. https://doi.org/10.1111/j.1749-6632.1999.tb09178.x.
56. McCall, A.A., Miller, D.M., DeMayo, W.M., Bourdages, G.H., and Yates, B.J. (2016). Vestibular nucleus neurons respond to hindlimb movement in the conscious cat. J. Neurophysiol. *116*, 1785–1794. https://doi.org/10.1152/jn.00414.2016.
57. Gdowski, G.T., and McCrea, R.A. (2000). Neck proprioceptive inputs to primate vestibular nucleus neurons. Exp. Brain Res. *135*, 511–526. https://doi.org/10.1007/s002210000542.
58. Sadeghi, S.G.M., Cullen, D.E., and K.E.. (2009). Different neural strategies for multimodal integration: comparison of two macaque monkey species. Exp. Brain Res. *95*, 45–57. https://doi.org/10.1007/s00221-009-1751-3.
59. Sadeghi, S.G., Minor, L.B., and Cullen, K.E. (2011). Multimodal integration after unilateral labyrinthine lesion: single vestibular nuclei neuron responses and implications for postural compensation. J. Neurophysiol. *105*, 661–673. https://doi.org/10.1152/jn.00788.2010.
60. Fujita, H., Kodama, T., and du Lac, S. (2020). Modular output circuits of the fastigial nucleus for diverse motor and nonmotor functions of the cerebellar vermis. eLife *9*, e58613. https://doi.org/10.7554/eLife.58613.
61. Gruver, K.M., Jiao, J.W.Y., Fields, E., Song, S., Sjöström, P.J., and Watt, A.J. (2024). Structured connectivity in the output of the cerebellar cortex. Nat. Commun. *15*, 5563. https://doi.org/10.1038/s41467-024-49339-1.
62. Dietrichs, E. (1983). The cerebellar corticonuclear and nucleocortical projections in the cat as studied with anterograde and retrograde transport of horseradish peroxidase. V. The posterior lobe vermis and the flocculonodular lobe. Anat. Embryol. (Berl) *167*, 449–462. https://doi.org/10.1007/BF00315681.
63. Bernard, J.F. (1987). Topographical organization of olivocerebellar and corticonuclear connections in the rat–an WGA-HRP study: I. Lobules IX, X, and the flocculus. J. Comp. Neurol. *263*, 241–258. https://doi.org/10.1002/cne.902630207.
64. Ikeda, Y., Noda, H., and Sugita, S. (1989). Olivocerebellar and cerebellolivary connections of the oculomotor region of the fastigial nucleus in the macaque monkey. J. Comp. Neurol. *284*, 463–488. https://doi.org/10.1002/cne.902840311.
65. Starr, M.S., and Summerhayes, M. (1983). Role of the ventromedial nucleus of the thalamus in motor behaviour–I. Effects of focal injections of drugs. Neuroscience *10*, 1157–1169. https://doi.org/10.1016/0306-4522(83)90106-9.
66. Goto, M., Swanson, L.W., and Canteras, N.S. (2001). Connections of the nucleus incertus. J. Comp. Neurol. *438*, 86–122. https://doi.org/10.1002/cne.1303.
67. Cornwall, J.C., Cooper, J.D., and Phillipson, O.T. (1990). Afferent and efferent connections of the laterodorsal tegmental nucleus in the rat. Brain Res. Bull. *25*, 271–284. https://doi.org/10.1016/0361-9230(90)90072-8.
68. Yakusheva, T.A., Shaikh, A.G., Green, A.M., Blazquez, P.M., Dickman, J.D., and Angelaki, D.E. (2007). Purkinje cells in posterior cerebellar vermis encode motion in an inertial reference frame. Neuron *54*, 973–985. https://doi.org/10.1016/j.neuron.2007.06.003.
69. Massot, C., Schneider, A.D., Chacron, M.J., and Cullen, K.E. (2012). The vestibular system implements a linear-nonlinear transformation in order to encode self-motion. PLoS Biol. *10*, e1001365. https://doi.org/10.1371/journal.pbio.1001365.
70. Carriot, J., Jamali, M., Chacron, M.J., and Cullen, K.E. (2017). The statistics of the vestibular input experienced during natural self-motion differ between rodents and primates. J. Physiol. *595*, 2751–2766. https://doi.org/10.1113/JP273734.
71. Cherif, S., Cullen, K.E., and Galiana, H.L. (2008). An improved method for the estimation of firing rate dynamics using an optimal digital filter. J. Neurosci. Methods *173*, 165–181. https://doi.org/10.1016/j.jneumeth.2008.05.021.
72. Carpenter, J., and Bithell, J. (2000). Bootstrap confidence intervals: when, which, what? A practical guide for medical statisticians. Stat. Med. *19*, 1141–1164. https://doi.org/10.1002/(sici)1097-0258(20000515)19:9<1141::aid-sim479>3.0.co;2-f.
73. Sylvestre, P.A., and Cullen, K.E. (1999). Quantitative analysis of abducens neuron discharge dynamics during saccadic and slow eye movements. J. Neurophysiol. *82*, 2612–2632. https://doi.org/10.1152/jn.1999.82.5.2612.
74. Cullen, K.E., Rey, C.G., Guitton, D., and Galiana, H.L. (1996). The use of system identification techniques in the analysis of oculomotor burst neuron spike train dynamics. J. Comput. Neurosci. *3*, 347–368. https://doi.org/10.1007/BF00161093.
75. Angelaki, D.E. (1993). Generation of two-dimensional spatial and temporal properties through spatiotemporal convergence between one-dimensional neurons. IEEE Trans. Bio Med. Eng. *40*, 686–692. https://doi.org/10.1109/10.237698.

Please cite this article in press as: Mildren et al., Convergence of vestibular and proprioceptive signals in the cerebellar nodulus/uvula enhances the encoding of self-motion in primates, Current Biology (2024), https://doi.org/10.1016/j.cub.2024.11.063

STAR★METHODS

KEY RESOURCES TABLE

REAGENT or RESOURCE	SOURCE	IDENTIFIER
Deposited data		
Raw and analyzed data	This paper	https://figshare.com/account/home#/projects/225963
Raw and analyzed data	Zobeiri and Cullen[42]	https://figshare.com/articles/dataset/eLife_2022_dataset/19362239?file=34388024
Experimental models: Organisms/strains		
Rhesus monkeys: Macaca mulatta	Johns Hopkins University	N/A
Software and algorithms		
Kilosort2.5		https://github.com/SpikeInterface/spikesorters/tree/master/spikesorters/kilosort2_5
Phy		https://github.com/cortex-lab/phy
Data Acquisition System, Intan RHS Stim/Recording system	Intan Technologies	https://www.intantech.com/RHS_system.html
Data Acquisition System, Cerebus Neural Signal Processor	Blackrock Microsystems	https://blackrockmicro.com/neuroscience-research-products/neural-data-acquisition-systems/cerebus-daq-system/
MATLAB 2020a	MathWorks	https://www.mathworks.com/products/matlab.html
Other		
128 channel Read-Write electrodes	Johns Hopkins University and Janelia HHMI	N/A

EXPERIMENTAL MODEL AND STUDY PARTICIPANT DETAILS

All experimental procedures were conducted with approval from the Johns Hopkins University Animal Care and Use Committee and adhered to the guidelines outlined by the United States National Institutes of Health (Protocol PR22M342). Cerebellar recordings were performed on one female and one male macaque monkeys (Macaca mulatta), weighing 7 and 12kg, respectively. A total of 63 recording sessions were performed. Throughout the course of the study, these animals were maintained in a controlled environment with a 12-hour light/dark cycle. Both macaque monkeys had previously participated in other research studies within our laboratory, exhibited overall good health, and did not require any medication throughout the course of this experiment.

METHOD DETAILS

Surgical procedures

The two macaque monkeys underwent aseptic surgical preparations for chronic extracellular recording following established protocols.[69] The animals received pre-anesthetic medications to ensure analgesia and muscle relaxation (ketamine hydrochloride (15 mg/kg i.m.), buprenorphine (0.01 mg/kg i.m.), and diazepam (1 mg/kg i.m.)). To reduce swelling and prevent infection, loading doses of dexamethasone (1 mg/kg i.m.) and cefazolin (50 mg/kg i.v.) were administered. To stabilize heart rate and reduce salivation, anticholinergic glycopyrrolate (0.005 mg/kg i.m.) was also administered before the surgery and every 2.5–3 hours throughout the surgical procedure. During the surgery, isoflurane gas (0.8–1.5%), combined with a minimum of 3 l/min of 100% oxygen, was administered and adjusted to achieve the desired level of anesthesia. Vital signs were monitored continuously throughout the surgical procedure, including heart rate, blood pressure, respiration, and body temperature.

During the surgical procedure, animals were implanted with a custom-made medical grade titanium head post for head fixation as well as recording chambers that allowed for targeting the posterior cerebellar vermis. In the first macaque, the positioning of the recording chambers was determined using stereotaxic targeting procedures, and a CT scan was performed post-implantation with guide tubes placed in the brain to evaluate targeting. In the second macaque, recording chambers were positioned based on the co-registration of a CT and MRI scan using Brainsight (Brainsight 2 Vet, Rogue Research, Montreal, Canada). Accurate placement of the recording chambers and targeting of neural structures was confirmed post-surgery by co-registration of a second CT scan. The implant was chronically fastened to the skull with titanium screws and Simplex P bone cement (Stryker Orthopedics, Mahwah, NJ). A craniotomy was carefully performed within the recording chamber to provide access to the brain. After the surgery, medications were delivered including dexamethasone (0.5 mg/kg i.m. for 4 days), anafen (2 mg/kg on the first day, 1 mg/kg on subsequent days), and buprenorphine (0.01 mg/kg i.m. every 12 hours for 2–5 days, depending on the animal's pain level. Cefazolin (25 mg/kg)

Please cite this article in press as: Mildren et al., Convergence of vestibular and proprioceptive signals in the cerebellar nodulus/uvula enhances the encoding of self-motion in primates, Current Biology (2024), https://doi.org/10.1016/j.cub.2024.11.063

was injected twice daily for 10 days to prevent infection. The animals were allowed a recovery period of 2 weeks before commencing any experimental procedures.

Experimental procedures

During the experiment, the monkey was seated in a primate chair secured on top of a turntable and linear sled. The head was fixed using a head post attached to a near-frictionless linear head sled that could allow for yaw rotation or translations of the head on the body in anteroposterior and mediolateral directions (Figure S1). First, we applied passive vestibular stimulation by translating the whole body in space (whole body condition). The motion profile we applied replays of those actively made by rhesus monkeys during voluntary orienting in natural conditions[36,70] The displacement of these motions were approximately 7cm, and peak velocity, acceleration, and jerk of these stimuli were approximately 0.18m/s, 1.2m/s^2, 30m/s^3. Next, we held the head stable and translated the body underneath the head to stimulate neck proprioceptors (body under head condition). Finally, we moved just the head to provide vestibular and neck proprioceptive stimulation concurrently (head on body condition). These conditions were tested both in the anteroposterior and mediolateral directions.

Next, in order to test whether NU Purkinje cell vestibular responses were modulated as a function of static head position, we applied the same naso-occipital vestibular stimulation using whole body translations while the head was statically rotated relative to the body at 3 different angles in the yaw axis (45° ipsilateral, 0° or straight ahead, and 45° contralateral). In a subset of recordings where neurons remained isolated, we tested two additional head positions: 22.5° ipsilateral and 22.5° contralateral. These above conditions were achieved by rotating the body underneath the head while keeping the whole body translation aligned with the naso-occiptal axis of the head.

Data acquisition

During these conditions, we recorded motion of the head using an 6D (3D linear acceleration and 3D angular velocity) IMU mounted on the head post, and motion of the chair using a 3D accelerometer. All analogue signals were sampled at 1kHz (Blackrock Microsystems). We recorded neural activity from the NU using 128 channel silicon read-write electrodes (IMEC). The 128 channels spanned a 1.6 mm recording area in a zig-zag pattern. Neural signals were amplified, bandpass filtered (0.1Hz-7.5kHz) and digitized by four 32-channel RHS stim/recording head stages (Intan technologies) and streamed by an RHS stim/recording controller (Intan technologies) at 30kHz. Spike sorting was performed by Kilosort v2.5 and further curated in Phy2. Only cell clusters that remained isolated single units across a set of paradigms were included in further analyses.

QUANTIFICATION AND STATISTICAL ANALYSIS

Head and body kinematic signals were low-pass filtered at 10 Hz. From recorded linear acceleration, we calculated velocity and jerk by integrating and differentiating the recorded acceleration signal, respectively. Each motion trial was segmented based on threshold crossings and all segments for each motion direction were aligned by peak jerk. Single unit spike times extracted from Kilosort and Phy were filtered with a kaiser window at a cutoff of 7 Hz to compute firing rate.[71] Linear least-squares regressions were performed to estimate each Purkinje cell's response to head motion using 3 terms: acceleration, velocity, and jerk.

$$\widehat{fr}(t) = b + S_v\dot{X}(t) + S_a\ddot{X}_i(t) + S_j\dddot{X}(t) \quad \text{(Equation 1)}$$

where $\widehat{fr}(t)$ is the estimated firing rate, b is a bias term, S_v, S_a, and S_j are coefficients representing the gains for velocity, acceleration, and jerk, respectively, and $\dot{X}$, $\ddot{X}$ and $\dddot{X}$ are head velocity, acceleration, and jerk, respectively. We used the same approach using body motion for the body under head condition, and head motion for the head on body condition. For each model coefficient in the analysis, we computed 95% confidence intervals using a nonparametric bootstrapping approach (2000 times with replacement[72,73]). All non-significant coefficients were set to zero. We then used these coefficients to estimate the sensitivity and phase of the response relative to acceleration using the following equations:

$$Sensitivity = sgn(S_j, S_a, S_{v,i}) \times \sqrt{\frac{\left((2\pi f)^2 S_j - S_v\right)^2 + (2\pi f S_a)^2}{(2\pi f)^2}} \quad \text{(Equation 2)}$$

$$Phase = tan^{-1}\left(\frac{(2\pi f)^2 S_j - S_v}{2\pi f S_a}\right) \quad \text{(Equation 3)}$$

Where the frequency of the stimulus was 1Hz (500ms half-cycle translations) and the sign terms were either +1 for positive coefficients or -1 for negative coefficients. Our simple linear summation model was generated by vector addition of the sensitivity and phase of vestibular and proprioceptive responses for each Purkinje cell. We compared sensitivity to vestibular, proprioceptive, combined stimulation, and model prediction using pairwise *t*-tests. Similarly, Pearson correlations were used to examine the relationship

Please cite this article in press as: Mildren et al., Convergence of vestibular and proprioceptive signals in the cerebellar nodulus/uvula enhances the encoding of self-motion in primates, Current Biology (2024), https://doi.org/10.1016/j.cub.2024.11.063

between the model prediction and actual sensitivity and phase to head on body motion, performed separately for the preferred and non-preferred direction of the Purkinje cells and for anteroposterior and mediolateral motion.

We classified neuron responses to vestibular and neck proprioceptive stimulation as either linear, rectifying, or v-shaped based on their firing rate response. Purkinje cells were deemed linear if they increased their firing rate in the preferred direction and decreased in the non-preferred direction, with a difference in the magnitude of their sensitivity within 8 sp/s / m/s^2. Purkinje cells were classified as rectifying if they increased their firing rate in the preferred direction with a minimum modulation of 8 sp/s / m/s^2, and had minimal modulation in the non-preferred direction (< 8 sp/s / m/s^2). Finally, Purkinje cells were classified as v-shaped if they showed a similar increase in firing rate in both directions (within 8 sp/s / m/s^2). Purkinje cells that did not fit any of these criteria were classified as other.

To assess the contribution of different kinematic terms (velocity, acceleration, and jerk) to each Purkinje cell's response, we also ran linear regression models with just two terms to assess the contribution of the missing term. We did this by calculating the decrease in the variance accounted for (VAF[74]) when the term of interest was removed from the model.

To estimate directional tuning preferences for vestibular and neck proprioceptive responses for Purkinje cells that were isolated across directions (anteroposterior and mediolateral), sensitivity tuning curves were calculated across angles using the equation:

$$S(\alpha) = \left[S^2_{ml}\cos^2\alpha + S^2_{ap}\sin^2\alpha + 2S_{ml}S_{ap}\sin\alpha\cos\alpha\cos(\Delta\varphi)\right]^{1/2} \quad \text{(Equation 4)}$$

Where $S(\alpha)$ is a Purkinje cell's sensitivity to stimulation applied at a given orientation α, and $\Delta\varphi$ is the difference between the phases of responses to anteroposterior and mediolateral translations.[75] Tuning direction preferences were compared between vestibular versus proprioceptive stimulation using a paired samples t-test.

We quantified head and body sensitivity ratios as each Purkinje cell's sensitivity to head on body translation divided by its sensitivity to whole body translation, and its sensitivity to body under head translation divided by its sensitivity to whole body translation, respectively. We then calculated a coding index by dividing the smaller value by the larger value of these two ratios. The tuning of vestibular responses as a function of static head on body position was quantified by fitting a Gaussian curve. In Purkinje cells that were not fit well by a Gaussian curve due to larger responses at one extreme, we fit a sigmoidal function.

We examined whether the integration of the firing rates across multiple Purkinje cells could predict responses of theoretical downstream target neurons (e.g., target neurons in the vestibular or fastigial nuclei[31,36]) that encode head or body motion using the following equation:

$$\widehat{Nu} = \sum_{i=1}^{N} w_i \times Pcell_i \quad \text{(Equation 5)}$$

Where $\widehat{Nu}$ is the firing rate response of a theoretical nucleus neuron that purely encoded either body motion only, or head motion only, and w_i is the weight of the influence of an individual Purkinje cell on this theoretical neuron, which was constrained to be non-positive due to the inhibitory nature of Purkinje cell output. $Pcell_i$ are the recorded simple spike firing rates of N Purkinje cells. For each population size (N), we calculated 95% confidence intervals for the model prediction and goodness of fit (R^2) using bootstrapping.